Int J Clin Exp Med 2019;12(3):2278-2289
www.ijcem.com /ISSN:1940-5901/IJCEM0085778

Original Article

Bioinformatic analysis of glioblastomas through data mining and integration of gene database contributions to screen hub genes and analysis of correlations

Li Yang, Na Han, Xiaoxi Zhang, Yangmei Zhou, Mengxian Zhang

Department of Oncology, Tongji Hospital, Tongji Medical College, Huazhong University of Science and Technology, Jiefang Road 1095, Wuhan 430030, PR China

Received September 20, 2018; Accepted November 8, 2018; Epub March 15, 2019; Published March 30, 2019

Abstract: Glioblastomas (GBM), having a poor prognosis, are some of the most aggressive intracranial tumors in adults. Through advances in bioinformatic analysis, precise candidate biomarkers can be screened out effectively. To explore hub genes and related signaling pathways of GBM, gene expression profiles were downloaded from The Cancer Genome Atlas (TCGA) dataset and Gene Expression Omnibus (GEO) datasets GSE15824 and GSE90886. Differentially expressed genes (DEGs) were identified using the Edger package in the R software. Gene Oncology (GO) and Kyoto Encyclopedia of Genes and Genomes (KEGG) enrichment analyses were performed for DEGs through the DAVID database. Subsequently, target genes were predicted using the Venn Diagram package in the R software. Next, correlation analysis of public database GSE15824 was examined to evaluate the correlation between expression of NDC80 and levels of other target genes. Finally, the R2: Genomics Analysis and Visualization Platform was probed to study the association of expression of NDC80, CDC45, KIF2C, WEE1, OIP5, CD74, PRKCG, and other hub genes with overall survival (OS) of patients with GBM. DEGs were mainly enriched in cell division, cell proliferation, mitotic cell cycle, epithelial to mesenchymal transition, P53, and MAPK signaling pathways. A total of 15 overlapping DEGs were screened among these 3 datasets. A total of 8 were certified to be related to prognosis of patients with GBM. NDC80 was significantly positively correlated with cell division and mitotic cell cycle markers CCNB1, NUF2, KNTC1, OIP5, WEE1, KIF2C and PLK1, but inversely related to OTUD7A. Therefore, functional and pathway enrichment analysis may reveal the pathogenesis and progression of GBM. NDC80, CDC45, KIF2C, WEE1, OIP5, CD74, PRKCG and WNT1 are expected to be important molecular targets for early diagnosis, therapeutics, and prognosis of patients with GBM.

Keywords: Bioinformatic analysis, glioblastoma, functional enrichment analysis, hub genes, correlation analysis, prognosis

Introduction

Glioblastomas (GBM) are the most common primary malignant tumors of the central nervous system in adults. This disease records a high recurrence rate and a peculiar mortality rate. Given their poor differentiation, rapid proliferation, and aggressive behavior, the median survival time of patients with this condition is only about 14 months, with very few long-term survivors [1]. Maximum surgical resection combined with radiation and chemotherapy, such as temozolomide, has not changed the trend of devastating progression. Therapy for GBM is difficult and the prognosis remains bleak. Etiologic diagnosis mainly depends on medical imaging and tissue biopsies of the nervous system, despite the existence of biomarkers, such as IDH1, ATRX, MGMT and PTEN, presented by recent studies for diagnosis of GBM. However, the specific molecular mechanisms of GBM are unclear. Currently, bioinformatic analysis can quickly and effectively screen out differentially expressed genes (DEGs) between tumor and normal tissues, offering an effective means for genome expression profile studies. Clinical data from databases can be utilized to obtain the relationship between target gene expression and patient prognosis. Data mining will provide important clinical value in searching for reliable

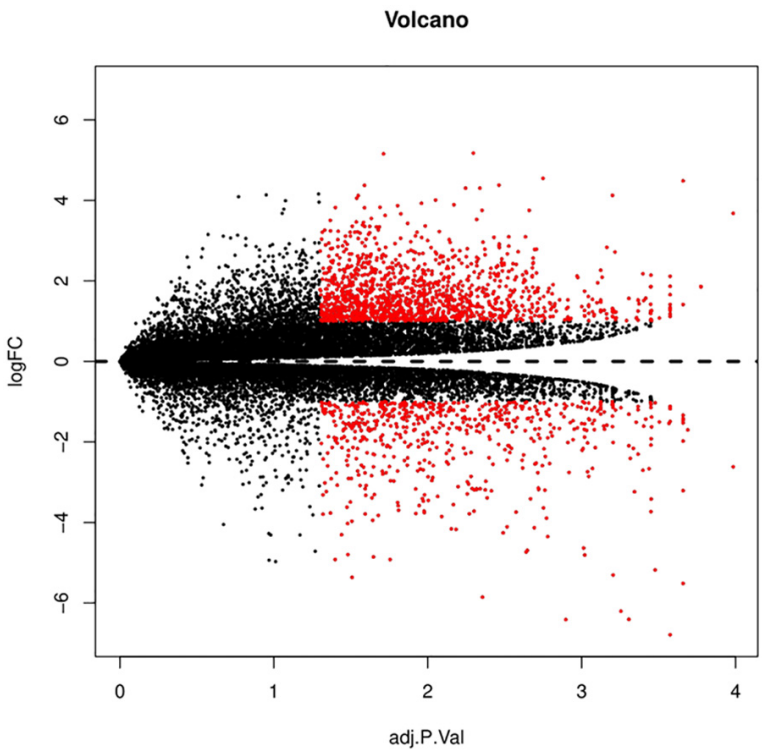

Figure 1. Volcano plots of the DEGs. Glioblastoma samples versus normal brain samples in GSE15824. P < 0.01, logFC (fold change) > 1.0 or logFC < -1.0 as the criteria.

therapeutic targets and prognostic indicators. It may open a new horizon in investigating progression and recurrence after GBM treatment.

Cancer Genome Atlas (TCGA) dataset and Gene Expression Omnibus (GEO) database are public repositories for data storage, freely available to researchers. These databases enable data mining of gene expression or clinical information profiles involved in the tumorigenesis and progression of diseases. In performing bioinformatic integration analysis of the gene microarray data of GBM downloaded from TCGA and GEO databases, the present study successfully obtained a set of DEGs, helping to identify the target of diagnosis, therapeutic, and prognosis of GBM.

In the present research, gene expression of GBMs and normal brain tissues was compared in TCGA, GSE15824, and GSE90886 GBM databases. A total of 15 DEGs that overlapped among these three datasets were screened out. Gene Ontology (GO) and Kyoto Encyclopedia of Genes and Genomes (KEGG) pathway enrichment analyses were further performed to identify DEGs using the Database for Annotation Visualization and Integrated Discovery (DAVID). This study further acknowledged the biological meaning behind the genes involved in GBM. NDC80, CDC45, KIF2C, PRKCG and WNT1, which are expected candidate hub genes, may serve as probable molecules participating in GBM cell mitosis, proliferation, cell cycle process, and malignant pathogenesis.

Materials and methods

Data processing and analysis

Gene expression and clinical information profiles of GBM were downloaded from the TCGA (https://cancergenome.nih.gov/) public dataset. Another two GBM gene expression profile datasets, GSE15824 and GSE90886, were obtained from the NCBI GEO database (https://www.ncbi.nlm.nih.gov/geo/). GPL570 (Affymetrix Human Genome U133 Plus 2.0 Array) and GPL 15207 (Affymetrix Human Gene Expression Array) are platforms of GEO datasets for GSE15824 and GSE90886. The expression chip of GBM, RNA-seq level-3 data, was downloaded from the TCGA dataset. A chip expression matrix file was generated and the Ensembl ID was converted into the gene name (Gene Symbol). Similarly, background correction and standardization of the GEO downloaded data were carried out using the RMA algorithm of the Affy package in the R software. The TCGA dataset contained 174 samples, including 169 GBM samples and 5 normal brain samples. In the GSE15824 dataset, 40 normal tissues and 5 tumor tissues were present. Another array data of GSE90886, consisting of 18 samples, was included, with 9 tumor tissues and 9 non-cancerous tissues.

Identification of DEGs

Original data of TXT files for was downloaded analysis. DEGs were identified with the Edger package (“https://bioconductor.org/

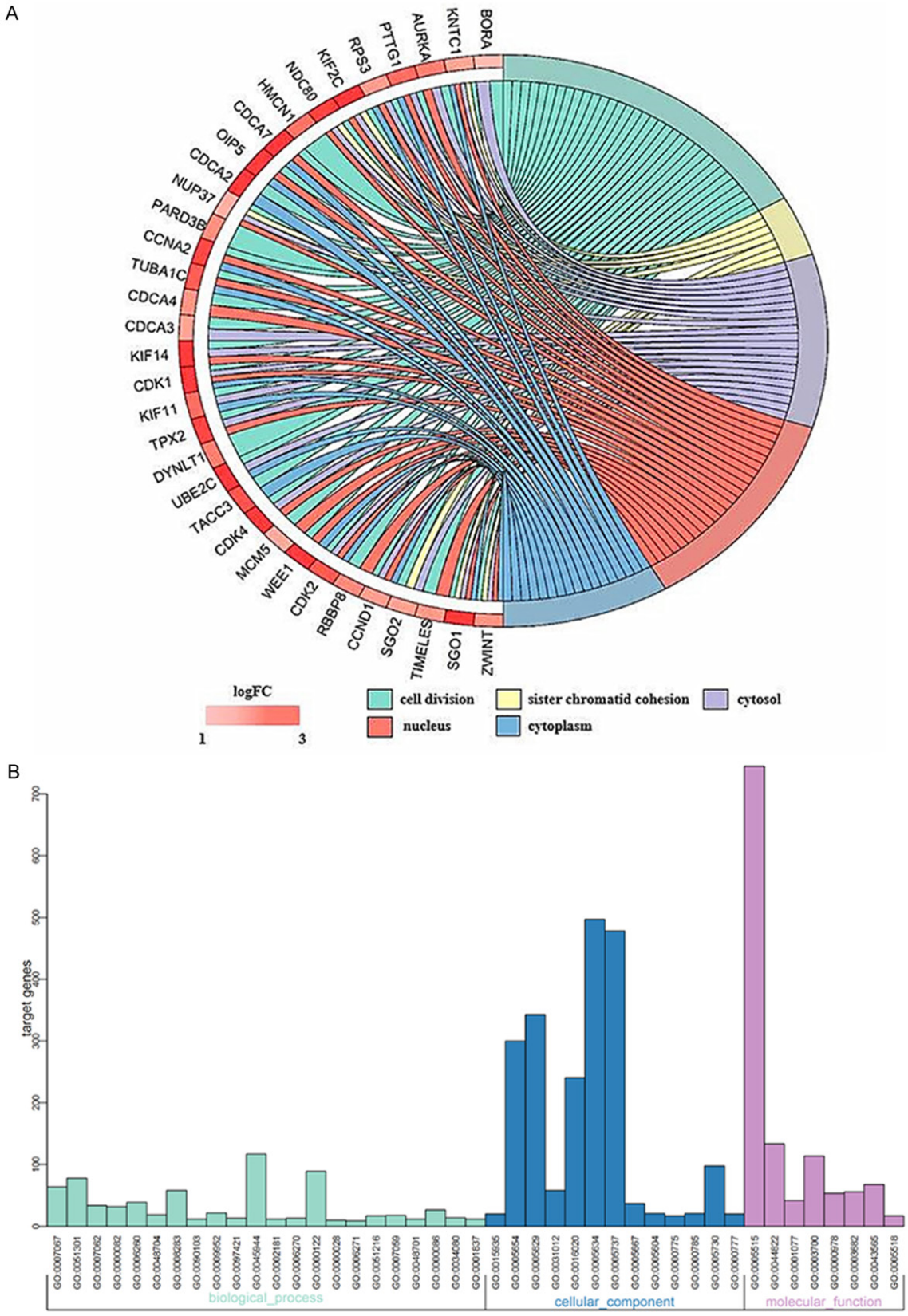
A
BORA
KNTC1
AURKA
PTTG1
RPS3
KIF2C
NDC80
HMCN1
CDCA7
OIP5
CDCA2
NUP37
PARD3B
CCNA2
TUBA1C
CDCA4
CDCA3
KIF14
CDK1
KIF11
TPX2
DYNLT1
UBE2C
TACC3
CDK4
MCM5
WEE1
CDK2
RBBP8
CCND1
SGO2
TIMELESS
SGO1
ZWINT
logFC
1
3
cell division
sister chromatid cohesion
cytosol
nucleus
cytoplasm
B
target genes
0
100
200
300
400
500
600
700
biological_process
cellular_component
molecular_function

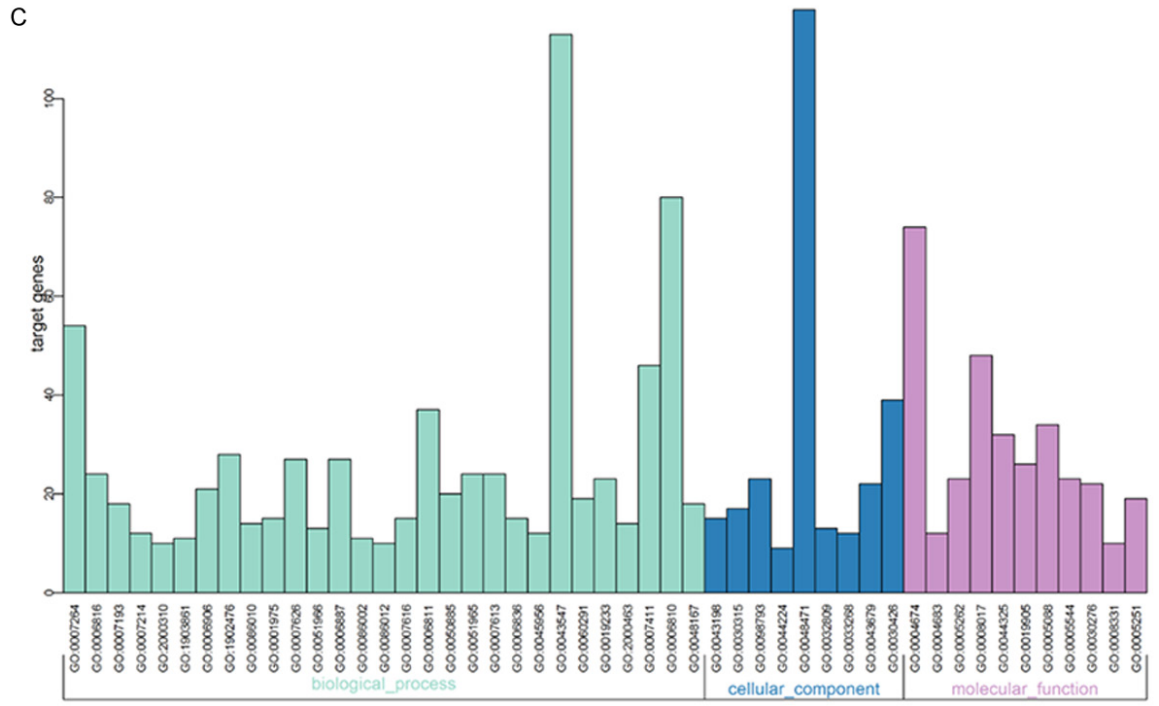

Figure 2. GO annotation of DEGs. (A) GO plot shows the top five GO annotations that are most significantly enriched in DEGs. Each bar in (B) (upregulated genes) and (C) (downregulated genes) represents a function of DEGs. The height of the bar represents the number of enriched DEGs. Green, blue, and purple indicate the biological processes (BP), cell composition (CC), and molecular function (MF) of the genes, respectively.

biocLite.R") in the R software. In GSE15824 and GSE90886, analysis was carried out using GEO2R (http://www.ncbi.nlm.nih.gov/geo/geo2r/), an efficient tool for processing raw submitter-supplied data tabulations, screening out DEGs between GBM and normal samples, and analyzing almost any GEO series by the limma R packages. The adjust *P*-value < 0.01 (FDR), |FC| (fold change) ≥ 2 was used as the criteria. Subsequently, a volcano plot was created using the DEGs (**Figure 1**).

Functional and pathway enrichment analysis

The DAVID online platform (version 6.7, https://david.ncifcrf.gov/) provides a series of function annotations in GO and pathway categories, allowing researchers to acknowledge the biological meaning behind the numerous core genes [2]. Gene functions can be categorized by GO annotation, including the biological process, molecular function, and cellular component. KEGG pathway enrichment analysis links genomic information with signal transduction and performs a higher-level systemic function. The list of DEGs was submitted to the DAVID website to identify corresponding GO functions and KEGG pathways. Finally, enrichment analysis results were visualized. The cut-off criterion for screening GO and KEGG categories was set as $P < 0.05$.

Prediction of target genes

Final target genes were predicted using the Venn Diagram package in the R software for screened DEGs. Target genes were common intersection genes gained from the top 2000 genes of each database (TCGA, GSE15824, and GSE90886). The remaining DEGs that could not be overlapped among the three databases were excluded.

Correlation analysis

Public dataset GSE15824 contained 35 brain tumor samples (12 primary GBMs, 3 secondary GBMs, 8 astrocytomas and 7 oligodendrogliomas), 5 GBM cell lines (LN018, LN215, LN229, LN319 and BS149), 2 normal brain tissue samples, and 3 normal human astrocytes. Therefore, GSE15824 was examined, evaluat-

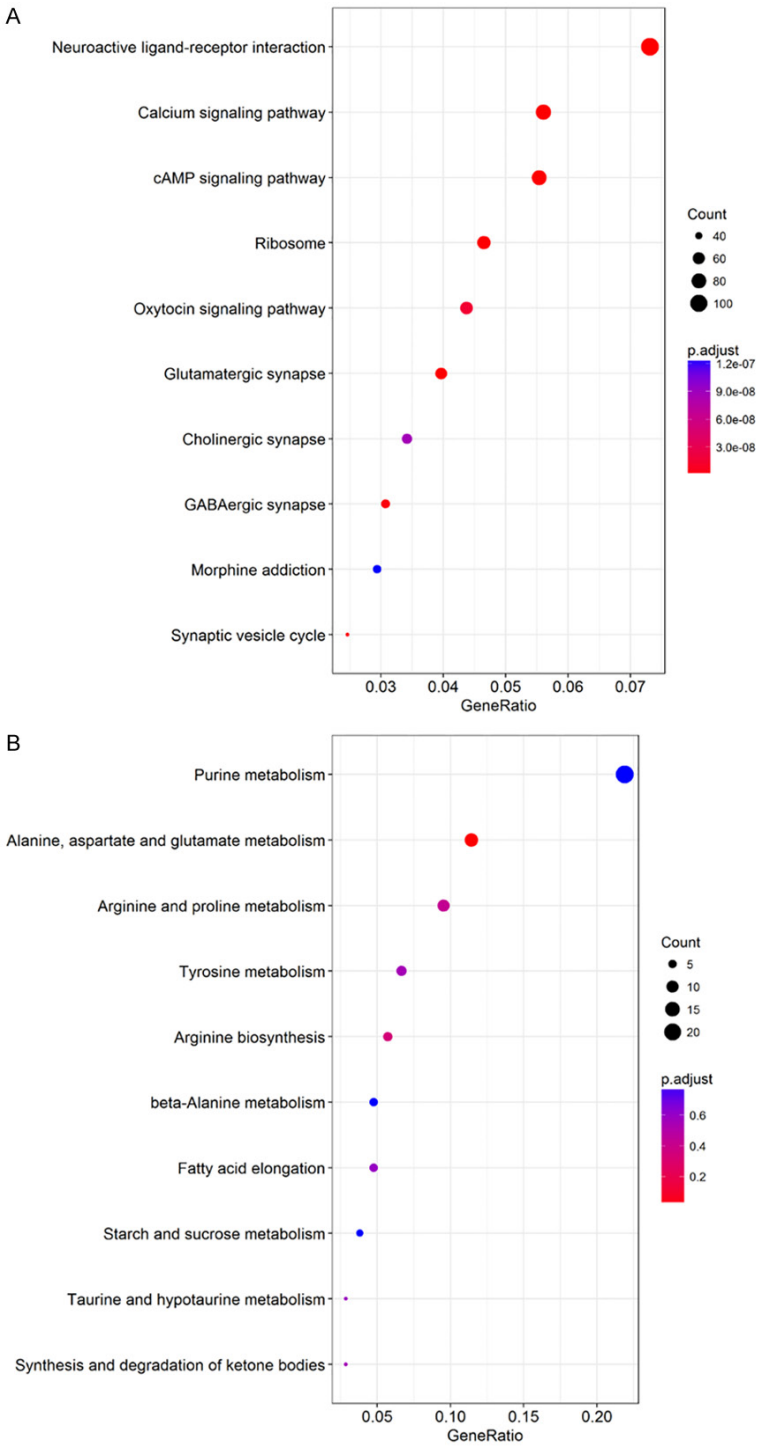

Figure 3. KEGG pathway enrichment of DEGs. Each dot in (A) (upregulated genes) and (B) (downregulated genes) represents a KEGG pathway. The size of each dot represents the number of genes enriched, whereas the color indicates the *P* value.

ing the correlation between expression of NDC80 and levels of the other remaining target genes in GBM tissues. Pearson's correlation coefficient analysis was used to determine correlations.

Survival analysis

The R2 was probed: Genomics Analysis and Visualization Platform (hgserver1.amc.nl/cgi-bin/r2/main.cgi) was used to study the association of NDC80, NUF2, PLK1, CDC45, PRKCG, WNT1, and other expressed hub genes with overall survival (OS) in patients with GBM. Kaplan-Meier analysis of the prognosis of patients with GBM was performed on the dataset downloaded from the TCGA database. Significance of difference tests on survival curves between the DEG groups were conducted by log-rank test.

Statistical analysis

In accordance with previous studies, SPSS 19.0 for Windows was used for all statistical analyses. Survival analysis was performed by Kaplan-Meier analysis and differences between groups were tested by log-rank test. *P* values < 0.05 indicate statistical significance.

Results

DEG identification

The gene expression profile was downloaded from the professional public database. Data manipulation, statistical analysis, and visualization were accomplished using R software. Results with |FC| ≥ 2 and *P*-value < 0.01 between GBM and normal samples were significant. Finally, 10,144 genes were selected as DEGs in the TCGA dataset, 5,153 genes (38.13%) of which were upregulated and 4,991 (61.87%) were downregulated. The information

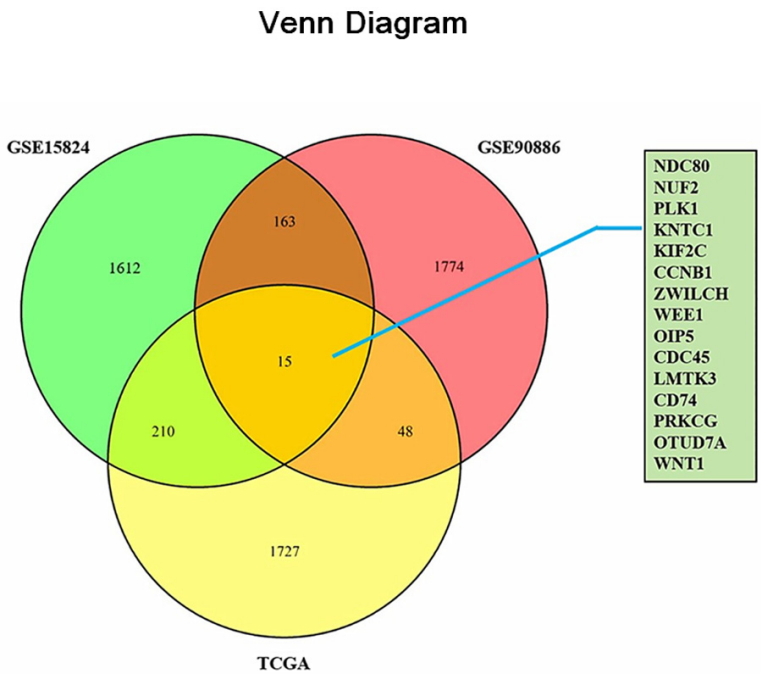

Figure 4. Venn chart of target genes in the database. Identification of the top 2,000 DEGs in the mRNA expression profiling datasets of TCGA, GSE15824, and GSE90886 that overlapped under analysis via Venn Diagram package in the R software. Fifteen overlapped DEGs, including NDC80, NUF2, PLK1, KNTC1, KIF2C, CCNB1, ZWILCH, WEE1, OIP5, CDC45, LMTK3, CD74, PRKCG, OTUD7A and WNT1, in these three datasets were selected.

Table 1. Hub gene expression in GBM (compared with normal brain tissues)

Gene	Up-/down-regulated	LogFC	*P* value	FDR
NDC80	Up	5.99	1.20E-09	3.92E-19
NUF2	Up	4.19	1.21E-11	1.62E-10
WNT1	Down	-4.33	5.41E-28	4.39E-26
CDC45	Up	5.61	4.88E-15	9.67E-14
PLK1	Up	3.29	5.48E-09	5.03E-08
KIF2C	Up	4.82	6.12E-15	1.20E-13
CCNB1	Up	2.93	1.20E-08	1.04E-07
LMTK3	Down	-2.59	4.31E-21	1.68E-19
ZWILCH	Up	1.022	0.003	0.017
KNTC1	Up	1.98	1.34E-06	8.36E-06
WEE1	Up	4.07	2.71E-19	8.49E-18
OIP5	Up	3.97	2.32E-11	3.00E-10
PRKCG	Down	-5.90	8.46E-47	6.91E-44
OTUD7A	Down	-3.52	1.66E-31	2.04E-29
CD74	Up	2.48	1.18E-05	6.14E-05

was available through GEO databases. In the GSE15824 dataset, 1,867 upregulated genes and 992 downregulated genes were detected. GSE90886 contained a total of 2,013 DEGs (1,369 upregulated genes and 644 downregulated genes). Data in GSE15824 were then presented as a volcano plot (**Figure 1**).

GO functional enrichment analysis

Figure 2A shows the top five GO annotations corresponding to the most significant enrichments of DEGs in the study. Of note, these genes were significantly enriched in the processes associated with cell division, sister chromatid cohesion, cytosol, nucleus, and cytoplasm. These genes may be involved in the tumorigenesis and progression of GBM. As shown in detail in **Figure 2B** and **2C**, the upregulated genes were mainly involved in biological processes and molecular function, including cell division (GO: 0051301), cell proliferation (GO: 0008283), mitotic cell cycle (GO: 0000082), positive/negative regulation of transcription from RNA polymerase II promoter (GO: 0045944/GO: 0000122), epithelial-to-mesenchymal transition (GO: 0001837), and protein binding (GO: 0005515). Additionally, the downregulated genes were mainly enriched in the positive regulation of GTPase activity (GO: 0043547), small GTPase-mediated signal transduction (GO: 0007264), axon guidance (GO: 0007411), ion transport (GO: 0006811), and protein serine/threonine kinase activity (GO: 0004674).

KEGG pathway enrichment analysis

The pathogenesis of tumors is a complex process. KEGG pathway analysis was enforced using DAVID to further show how DEGs distinguished functions may correlate with GBM genesis and progress. Neuroactive ligand-receptor interaction (hsa04080), GABAergic synapse (hsa04727), cAMP signaling pathway (hsa04024), the cell cycle (hsa04110), cellular senescence (hsa04218), P53 signaling pathway (hsa04115), and Ras and MAPK signaling pathways (hsa04010) were represented in

upregulated genes. DEGs showing distinguished functions may be correlated with cancer genesis and progression. Occasionally, the KEGG pathway was recognized as insignificant for downregulated genes when $P < 0.05$ (**Figure 3A** and **3B**).

Target genes in the database

The Venn Diagram package in the R software was used to predict final target genes. The top 2000 genes of each database (TCGA, GSE15824, and GSE90886) were included in the selection criteria. Remaining DEGs that could not be overlapped among the three databases were excluded. A total of 15 genes, including NDC80, NUF2, WNT1, CDC45, PLK1, KIF2C, CCNB1, LMTK3, ZWILCH, KNTC1, WEE1, OIP5, PRKCG, OTUD7A and CD74, were overlapped among the three datasets (**Figure 4**). Of these genes, NDC80, NUF2, PLK1, KNTC1, KIF2C, CCNB1, ZWILCH, WEE1, OIP5, CDC45, LMTK3 and CD74 were upregulated, whereas PRKCG, OTUD7A, and WNT1 were downregulated. Expression fold-change levels of DEG mRNAs in the GBM tissues showed extremely significant differences from levels of normal brain tissues. These changes are demonstrated in **Table 1**.

Correlation between expression levels of target genes

A total of 15 hub genes were used to evaluate and certify whether they were correlated with cell division and mitotic cell cycle in GBM tissues. Correlation analysis of the public dataset GSE15824 showed that NDC80 mRNA expression was positively correlated with CCNB1 significantly ($R = 0.944$, $P < 0.05$), NUF2 ($R = 0.933$, $P < 0.05$), KNTC1 ($R = 0.929$, $P < 0.05$), OIP5 ($R = 0.926$, $P < 0.05$), WEE1 ($R = 0.92$, $P < 0.05$), KIF2C ($R = 0.894$, $P < 0.05$) and PLK1 ($R = 0.766$, $P < 0.05$), but inversely correlated with OTUD7A ($R = -0.855$, $P < 0.05$). NDC80 was found parallel with CDC45 ($R = 0.569$, $P > 0.05$), LMTK3 ($R = 0.273$, $P > 0.05$), WNT1 ($R = -0.113$, $P > 0.05$), CD74 ($R = -0.181$, $P > 0.05$) and PRKCG ($R = -0.277$, $P > 0.05$), but the relationship between NDC80 and ZWILCH could not be evaluated (**Figure 5A-C**).

Prognostic value of hub genes

Hub genes screened in this paper were differentially expressed in GBM. To further clarify the relationship between expression levels and prognosis of GBM, the R2: Genomics Analysis and Visualization Platform was used to analyze the association between expression of hub genes expression and the OS of patients with GBM. The clinical dataset was downloaded from 540 samples in the TCGA dataset. From this dataset, 36 patients lacking survival follow-up information were not included in the analysis. Hub genes used for survival analysis were divided into high- and low-expression groups. For the upregulated genes NDC80, CDC45, KIF2C, WEE1, OIP5 and CD74, this study recognized the 2-year survival rates of the high-expression groups to be 18%, 20%, 19%, 8%, 19% and 16%, respectively, whereas those of the low-expression groups were 35%, 48%, 29%, 23%, 37%, and 28%, respectively, ($P = 0.012$, $P = 0.042$, $P = 0.026$, $P = 0.0019$, $P = 0.0052$, $P = 0.014$, respectively). The 2-year survival rates of patients in the high-expression group of downregulated genes PRKCG and WNT1 were 27% and 25%, whereas those of the low-expression group were only 13% and 14%, respectively. Present findings demonstrate that the prognosis of the high-expression group of PRKCG and WNT1 was significantly better than that of the low-expression group ($P = 0.0017$, $P = 0.0011$) (**Figure 6**).

Discussion

GBMs are an aggressive malignancy of the brain, characterized by highly invasive and rapid growth. Morbidity has increased yearly, especially among middle-aged and elderly people. The prognosis remains poor despite comprehensive therapy. The pathogenesis and progression of malignancies are driven by specific genetic and epigenetic changes, comprising a complex biological process. Recently, with the rise of various high-throughput techniques, a series of cancer microarray expression profiles and whole-genome sequencing technology have been widely used to explore the biology or genetic variation of malignant tumors, aiming to understand the disease accurately.

The present work initially obtained DEGs between GBM and normal brain tissue samples from the TCGA dataset and GSE15824 and GSE90886 databases. GO functional and KEGG pathway enrichment analysis were performed to identify DEGs in the biological progression of GBM through the DAVID online

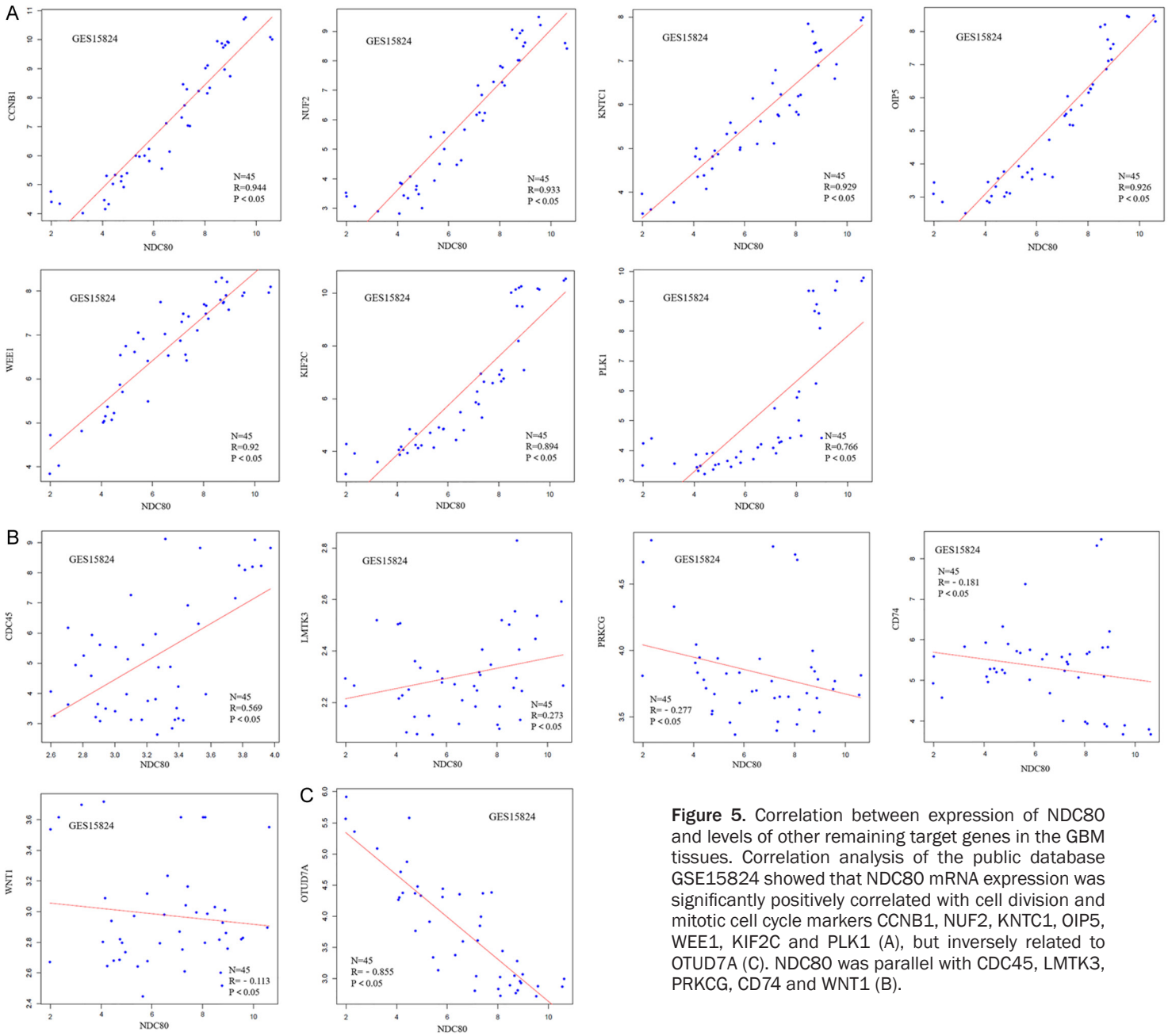

Figure 5. Correlation between expression of NDC80 and levels of other remaining target genes in the GBM tissues. Correlation analysis of the public database GSE15824 showed that NDC80 mRNA expression was significantly positively correlated with cell division and mitotic cell cycle markers CCNB1, NUF2, KNTC1, OIP5, WEE1, KIF2C and PLK1 (A), but inversely related to OTUD7A (C). NDC80 was parallel with CDC45, LMTK3, PRKCG, CD74 and WNT1 (B).

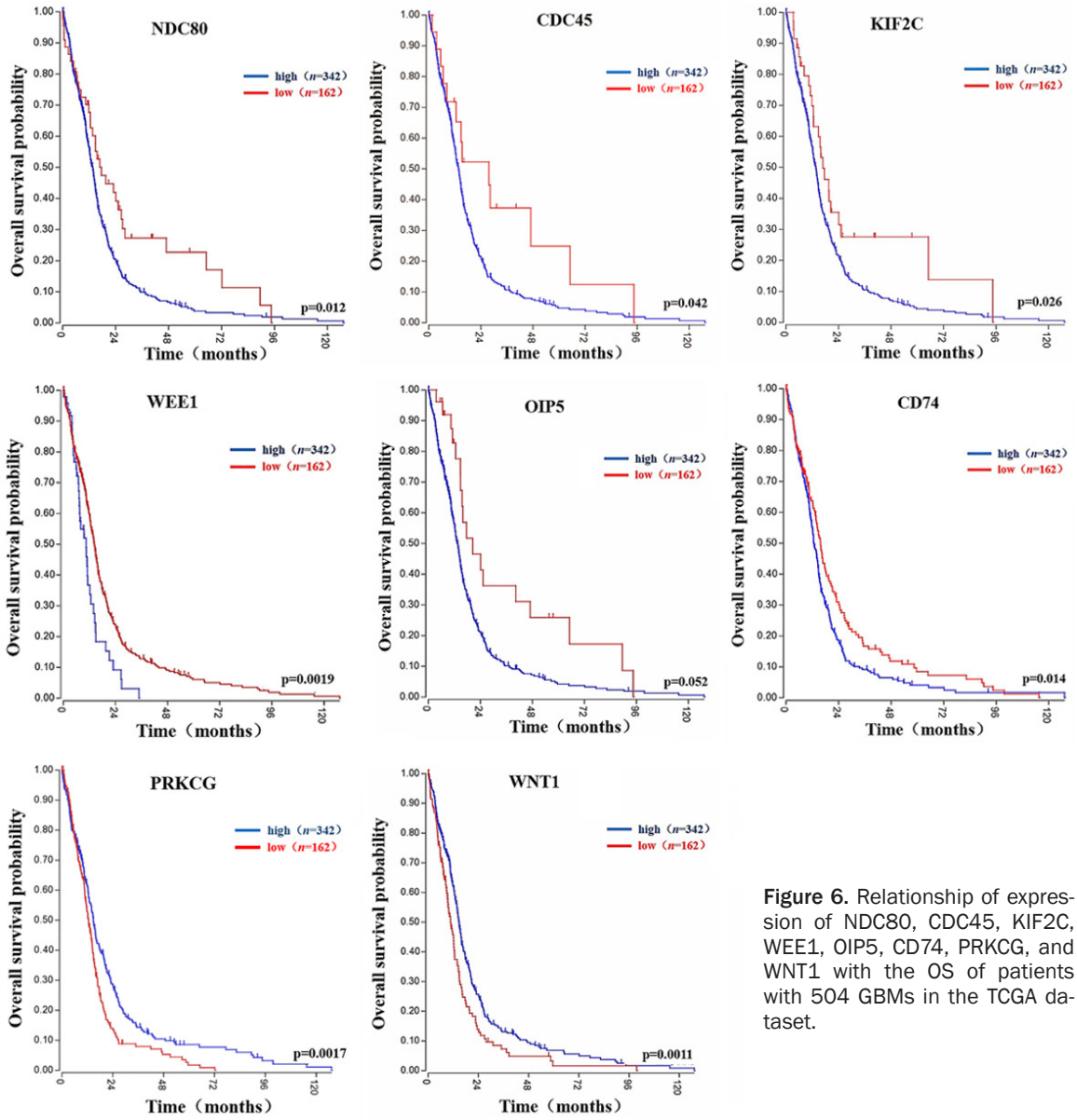

Figure 6. Relationship of expression of NDC80, CDC45, KIF2C, WEE1, OIP5, CD74, PRKCG, and WNT1 with the OS of patients with 504 GBMs in the TCGA dataset.

software. These upregulated genes were mainly involved in cell division, cell proliferation, the mitotic cell cycle, epithelial-to-mesenchymal transition and protein binding, cAMP, P53, and Ras and MAPK signaling pathways, all of which are closely related to GBM malignancy. Moreover, downregulated genes were mainly involved in the positive regulation of GTPase activity, small GTPase-mediated signal transduction, axon guidance, ion transport, protein serine/threonine kinase activity, and so forth. Of these genes, 15 hub genes overlapped among the three databases. Subsequently, correlation analysis of the hub genes showed that NDC80 was significantly positively correlated with CCNB1, NUF2, KNTC1, OIP5, WEE1, KIF2C and PLK1, while inversely associated with OTUD7A.

Regarding the clinical significance of these hub genes to GBM, survival curves demonstrated that upregulated genes NDC80, CDC45, KIF2C, WEE1, OIP5 and CD74 were significantly correlated with poor OS of patients with GBM. The high-expression group of downregulated genes, PRKCG and WNT1, showed better prognosis, as expected.

NDC80 (nuclear division cycle 80), also called Hec1, positively affects the mediation of spin-

dle assembly checkpoint signaling and helps maintain chromosome alignment stability during mitosis and chromosome segregation. The mitotic regulator NDC80 is associated with progression of various human malignancies, including hepatocellular carcinoma, colorectal cancer, osteosarcoma, and malignant pleural mesothelioma [3-6]. NUF2 is an essential element of the kinetochore-associated NDC80 complex with Spc24 and Spc25. This complex is required for kinetochore-microtubule attachment in mitosis [7]. Certainly, NDC80 is positively correlated with NUF2, supporting present findings. Trials have identified that silencing NUF2 inhibits cell proliferation in osteosarcomas [8]. As pivotal mitotic regulators, PLK1 and CCNB1 play a central role in promoting the activation of CDK1 with the help of phosphorylation by the positive regulator CDC25C, inhibiting the negative regulator WEE1 at the G2/M transition of the mitotic cell cycle [6, 9]. Overexpression of PLK1 and CCNB1 has been correlated with cancer cell proliferation, apoptosis, and lowered OS rates. It is a promising target for chemotherapy of oral cancer, ovarian cancer, and head and neck cancer [10-12]. WEE1 negatively regulates the G2/M cell cycle checkpoint, which is a critical mechanism for DNA repair in tumor cells that can confer resistance to DNA-damaging agents [13]. Using WEE1 inhibitors as chemosensitizers for DNA-targeted therapy may carry an important clinical significance. As another member of the mitotic checkpoint, KNTC1 (kinetochore associated 1) plays the role of preventing cells from prematurely exiting mitosis. This function relies on KNTC1's association with the mitotic RZZ complex. Kim found that mutations of KNTC1 contribute to the development of gastric and colorectal cancer by deregulating cell cycle and DNA damage signaling/repair [14]. GO annotations related to KIF2C include ATPase activity and microtubule motor activity. KIF2C is particularly enriched at the spindle midzone during mitosis and contributes to proper spindle formation, correction of aberrant attachments of microtubules to chromosomes, and chromosome segregation [15, 16]. KIF2C is a potential independent prognostic marker for patients with glioma and esophageal squamous cell carcinomas [17, 18]. OIP5 localizes to centromeres and contributes to chromosome segregation properly during cell division. Its other related pathways include chromosome maintenance and mitotic cell cycle. OIP5 is upregulated in expression in several cancers and is, therefore, a putative therapeutic target.

OTUD7A (OTU deubiquitinase 7A) is a deubiquitinizing enzyme vital to the development and function of the central nervous system [19, 20]. The encoded protein acts on RAF6 (TNF receptor-associated factor 6) to negatively regulate I-kappaB kinase/NF-kappaB signaling. OTUD7A is a possible tumor suppressor, downregulated by SNAIL1, in hepatocellular carcinoma cells, thus contributing to hepatocellular cancer progression and malignancy.

CDC45 (cell division cycle protein 45) is an essential component of the eukaryotic replicative DNA helicase. It is required for DNA synthesis during genome duplication [21, 22]. CDC45 has been reported to be a candidate oncogene in papillary thyroid carcinoma and cervical cancer because of overexpression and regulation of tumor progression [23, 24]. CD74 is an important chaperone that regulates antigen presentation for immune response. It is associated with the class II major histocompatibility complex. In brain metastasis, the tumor cell HLA class II peptidome complex can be regulated by CD74 [25]. In breast carcinoma patients, CD74 may be a useful prognostic marker that predicts poor outcomes [26]. In the present study, CDC45 and CD74 were upregulated in GBM. Prognosis of the high-expression group worsened. Genes are highly expressed in various types of tumor cells and participate in a series of biological processes, but their biological function in GBM remains elusive.

PRKCG (protein kinase C gamma) is a component of the PKC family and only expressed in the nervous system. PRKCG is involved in GBM progression-associated processes and has been inferred to affect the prognosis of GBM by influencing the MAPK signaling pathways [27].

WNT1 can encode secreted signaling proteins involved in tumorigenesis and several developmental processes, such as the regulation of cell fate, embryogenesis, and CNS development [28, 29]. WNT1 has been reported to target miR-185 to inhibit colon cancer cell proliferation and invasion, serving as a tumor suppressor and prognostic factor [30]. However, WNT1 can also regulate β-catenin signal path-

ways as a possible promoting factor of cell differentiation in various cancers [31, 32]. Therefore, it was speculated that the anomalous expression of a single gene is often accompanied by a chain of abnormal reactions of WNT1's downstream drive genes. This occurrence is an important reason explaining why the WNT1 abnormality can promote the development of various cancers.

Collectively, abnormal mitosis, chromosomal aberrations, cell cycle arrest, and malignant transformation may correlate with abnormal expression of NDC80, NUF2, PLK1, CCNB1, KIF2C, KNTC1, OIP5 and WEE1. Although the specific coordination mechanisms of proper chromosome segregation in cell division are indeterminate, abnormal expression of these genes is involved in cancer development and progression, to some extent. The oncogenic properties of dividing cell cycle progressions support present findings.

In conclusion, oncogenesis results from uncontrolled cell proliferation caused by the accumulation of polygenic aberration or abnormal expression. Data mining and integration help find potential biomarkers, signaling pathways, and prognostic indicators for GBM. These gene profiles should be applied in clinical research to analyze gene prognostic values in patients with GBM in future studies. Bioinformatic analysis is expected to provide new insight into the molecular mechanisms of GBM.

Acknowledgements

We acknowledge that this study was, in part, supported by a grant from the National Natural Sciences Foundation of China (No. 81772680). The authors are grateful to all study participants.

Disclosure of conflict of interest

None.

Address correspondence to: Dr. Mengxian Zhang, Department of Oncology, Tongji Hospital, Tongji Medical College, Huazhong University of Science and Technology, Jiefang Road 1095, Wuhan 430030, PR China. Tel: 0086-15827165669; Fax: 430030; E-mail: zhangmx73@163.com

References

[1] Delgado-Lopez PD, Corrales-Garcia EM. Survival in glioblastoma: a review on the impact of treatment modalities. Clin Transl Oncol 2016; 18: 1062-1071.

[2] Kouskoumvekaki I, Shublaq N, Brunak S. Facilitating the use of large-scale biological data and tools in the era of translational bioinformatics. Brief Bioinform 2014; 15: 942-952.

[3] Ju LL, Chen L, Li JH, Wang YF, Lu RJ, Bian ZL and Shao JG. Effect of NDC80 in human hepatocellular carcinoma. World J Gastroenterol 2017; 23: 3675-3683.

[4] Yan X, Huang L, Liu L, Qin H and Song Z. Nuclear division cycle 80 promotes malignant progression and predicts clinical outcome in colorectal cancer. Cancer Med 2018; 7: 420-432.

[5] Xu B, Wu DP, Xie RT, Liu LG and Yan XB. Elevated NDC80 expression is associated with poor prognosis in osteosarcoma patients. Eur Rev Med Pharmacol Sci 2017; 21: 2045-2053.

[6] Linton A, Cheng YY, Griggs K, Schedlich L, Kirschner MB, Gattani S, Srikaran S, Chuan-Hao Kao S, McCaughan BC, Klebe S, Van Zandwijk N and Reid G. An RNAi-based screen reveals PLK1, CDK1 and NDC80 as potential therapeutic targets in malignant pleural mesothelioma. Br J Cancer 2018; 118: e13.

[7] Sundin LJ, Guimaraes GJ, Deluca JG. The NDC80 complex proteins Nuf2 and Hec1 make distinct contributions to kinetochore-microtubule attachment in mitosis. Mol Biol Cell 2011; 22: 759-768.

[8] Fu HL, Shao L. Silencing of NUF2 inhibits proliferation of human osteosarcoma Saos-2 cells. Eur Rev Med Pharmacol Sci 2016; 20: 1071-1079.

[9] Kreis NN, Friemel A, Zimmer B, Roth S, Rieger MA, Rolle U, Louwen F, Yuan J. Mitotic p21Cip1/CDKN1A is regulated by cyclin-dependent kinase 1 phosphorylation. Oncotarget 2016; 7: 50215-50228.

[10] Vittal K, Pandian SS, Joseph LD and Raj SG. Immunohistochemical expression of polo-like kinase 1 in oral squamous cell carcinoma and oral submucous fibrosis. Indian J Dent Res 2018; 29: 171-175.

[11] Chong T, Sarac A, Yao CQ, Liao L, Lyttle N, Boutros PC, Bartlett JMS, Spears M. Deregulation of the spindle assembly checkpoint is associated with paclitaxel resistance in ovarian cancer. J Ovarian Res 2018; 11: 27.

[12] De Boer DV, Martens-de Kemp SR, Buijze M, Stigter-van Walsum M, Bloemena E, Dietrich R, Leemans CR, Van Beusechem VW, Braakhuis BJM, Brakenhoff RH. Targeting PLK1 as a novel chemopreventive approach to eradicate preneoplastic mucosal changes in the head and neck. Oncotarget 2017; 8: 97928-97940.

[13] Matheson CJ, Casalvieri KA, Backos DS and Reigan P. Development of potent pyrazolopyrimidinone based WEE1 inhibitors with limited

single-agent cytotoxicity for cancer therapy. ChemMedChem 2018; 13: 1897-1902.
[14] Kim YR, Chung NG, Kang MR, Yoo NJ and Lee SH. Novel somatic frameshift mutations of genes related to cell cycle and DNA damage response in gastric and colorectal cancers with microsatellite instability. Tumori 2010; 96: 1004-1009.
[15] Vogt E, Sanhaji M, Klein W, Seidel T, Wordeman L and Eichenlaub-Ritter U. MCAK is present at centromeres, midspindle and chiasmata and involved in silencing of the spindle assembly checkpoint in mammalian oocytes. Mol Hum Reprod 2010; 16: 665-684.
[16] Sanhaji M, Friel CT, Kreis NN, Krämer A, Martin C, Howard J, Strebhardt K and Yuan J. Functional and spatial regulation of mitotic centromere-associated kinesin by cyclin-dependent kinase 1. Mol Cell Biol 2010; 30: 2594-2607.
[17] Duan H, Zhang X, Wang FX, Cai MY, Ma GW, Yang H, Fu JH, Tan ZH, Fu XY, Ma QL, Wang XY and Lin P. KIF-2C expression is correlated with poor prognosis of operable esophageal squamous cell carcinoma male patients. Oncotarget 2016; 7: 80493-80507.
[18] Bie L, Zhao G, Wang YP and Zhang B. Kinesin family member 2C (KIF2C/MCAK) is a novel marker for prognosis in human gliomas. Clin Neurol Neurosurg 2012; 14: 356-360.
[19] Uddin M, Unda BK, Kwan V, Holzapfel NT, White SH, Chalil L, Woodbury-Smith M, Ho KS, Harward E, Murtaza N, Dave B, Pellecchia G, D'Abate L, Nalpathamkalam T, Lamoureux S, Wei J, Speevak M, Stavropoulos J, Hope KJ, Doble BW, Nielsen J, Wassman ER, Scherer SW and Singh KK. OTUD7A regulates neurodevelopmental phenotypes in the 15q13.3 microdeletion syndrome. Am J Hum Genet 2018; 102: 278-295.
[20] Shinawi M, Schaaf CP, Bhatt SS, Xia Z, Patel A, Cheung SW, Lanpher B, Nagl S, Herding HS, Nevinny-Stickel C, Immken LL, Patel GS, German JR, Beaudet AL and Stankiewicz P. A small recurrent deletion within 15q13.3 is associated with a range of neurodevelopmental phenotypes. Nat Genet 2009; 41: 1269-1271.
[21] Szambowska A, Tessmer I, Prus P, Schlott B, Pospiech H, Grosse F. Cdc45-induced loading of human RPA onto single-stranded DNA. Nucleic Acids Res 2017; 45: 3217-3230.
[22] Simon AC, Sannino V, Costanzo V and Pellegrini L. Structure of human Cdc45 and implications for CMG helicase function. Nat Commun 2016; 7: 11638.
[23] Zhang YX, Zhao YL. Pathogenic network analysis predicts candidate genes for cervical cancer. Comput Math Methods Med 2016; 2016: 3186051.
[24] Sun J, Shi R, Zhao S, Li X, Lu S, Bu H, Ma X. Cell division cycle 45 promotes papillary thyroid cancer progression via regulating cell cycle. Tumor Biology 2017; 39: 568835162.
[25] Zeiner PS, Zinke J, Kowalewski DJ, Bernatz S, Tichy J, Ronellenfitsch MW, Thorsen F, Berger A, Forster MT, Muller A, Steinbach JP, Beschorner R, Wischhusen J, Kvasnicka HM, Plate KH, Stefanović S, Weide B, Mittelbronn M and Harter PN. CD74 regulates complexity of tumor cell HLA class II peptidome in brain metastasis and is a positive prognostic marker for patient survival. Acta Neuropathol Commun 2018; 6: 18.
[26] Hasby EA, Khalifa RA. Expression of CD74 in invasive breast carcinoma: its relation to Nottingham prognostic index, hormone receptors, and HER2 immunoprofile. Tumori 2017; 103: 193-203.
[27] Zhang Y, Xu J, Zhu X. A 63 signature genes prediction system is effective for glioblastoma prognosis. Int J Mol Med 2018; 41: 2070-2078.
[28] Panigrahi I, Didel S, Kirpal H, Bellampalli R, Miyanath S, Mullapudi N and Rao S. Novel mutation in a family with WNT1-related osteoporosis. Eur J Med Genet 2018; 61: 369-371.
[29] Aldinger KA, Mendelsohn NJ, Chung BH, Zhang W, Cohn DH, Fernandez B, Alkuraya FS, Dobyns WB, Curry CJ. Variable brain phenotype primarily affects the brainstem and cerebellum in patients with osteogenesis imperfecta caused by recessive WNT1 mutations. J Med Genet 2016; 53: 427-430.
[30] Zhang W, Sun Z, Su L, Wang F, Jiang Y, Yu D, Zhang F, Sun Z and Liang W. miRNA-185 serves as a prognostic factor and suppresses migration and invasion through Wnt1 in colon cancer. Eur J Pharmacol 2018; 825: 75-84.
[31] Okuda Y, Nakano K, Suzuki K, Sugita Y, Kubo K, Maeda H, Okafuji N, Hasegawa H and Kawakami T. Wnt signaling as a possible promoting factor of cell differentiation in pleomorphic adenomas. Int J Med Sci 2014; 11: 971-978.
[32] Pai SG, Carneiro BA, Mota JM, Costa R, Leite CA, Barroso-Sousa R, Kaplan JB, Chae YK and Giles FJ. Wnt/beta-catenin pathway: modulating anticancer immune response. J Hematol Oncol 2017; 10: 101.